AD-A163 754 THE BIMOLECULAR REACTIONS OF OXIDIZING AGENTS WITH FREE 1/1
RADICALS OF THE F..(U) UNIVERSITY OF SOUTHERN
CALIFORNIA LOS ANGELES DEPT OF CHEMIST.. J CHOU ET AL.
UNCLASSIFIED 20 NOV 85 ARO-19095.3-CH DAAG29-82-K-0118 F/G 7/5 NL

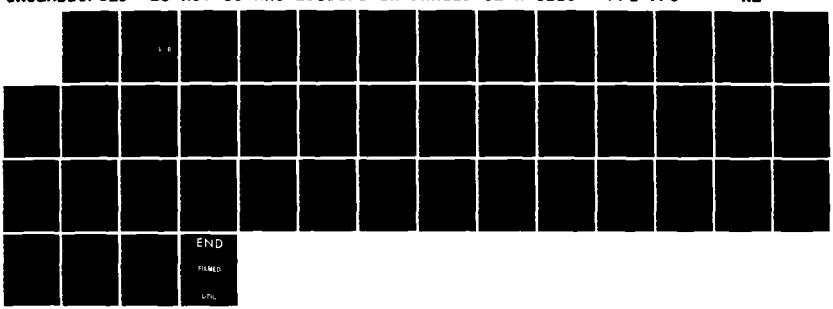

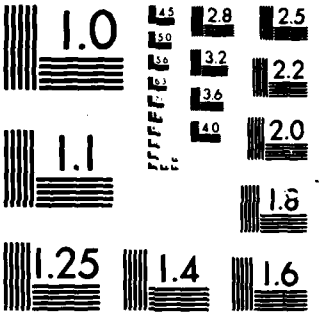

MASTER COPY - FOR REPRODUCTION PURPOSES

(2)

AD-A163 754

(When Data Entered)

NTATION PAGE	READ INSTRUCTIONS BEFORE COMPLETING FORM

1. REPORT NUMBER	2. GOVT ACCESSION NO.	3. RECIPIENT'S CATALOG NUMBER
ARO 19095.3-CH	N/A	N/A

4. TITLE (and Subtitle)	5. TYPE OF REPORT & PERIOD COVERED
The bimolecular reactions of oxidizing agents with free radicals of the form PX: The role of complex nuclear motion	FINAL REPORT 5/1/82-4/30/85
	6. PERFORMING ORG. REPORT NUMBER
7. AUTHOR(s)	8. CONTRACT OR GRANT NUMBER(s)
Jim-Son Chou, David Sumida, and Curt Wittig	DAAG29-82-K-0118
9. PERFORMING ORGANIZATION NAME AND ADDRESS	10. PROGRAM ELEMENT, PROJECT, TASK AREA & WORK UNIT NUMBERS
University of Southern California Chemistry Department Los Angeles, CA 90089-0484	N/A
11. CONTROLLING OFFICE NAME AND ADDRESS	12. REPORT DATE
U. S. Army Research Office Post Office Box 12211 Research Triangle Park, NC 27709	11/20/85
	13. NUMBER OF PAGES 40
14. MONITORING AGENCY NAME & ADDRESS(if different from Controlling Office)	15. SECURITY CLASS. (of this report) Unclassified
	15a. DECLASSIFICATION/DOWNGRADING SCHEDULE

16. DISTRIBUTION STATEMENT (of this Report)

Approved for public release; distribution unlimited.

DTIC ELECTE FEB 10 1986 S D

17. DISTRIBUTION STATEMENT (of the abstract entered in Block 20, if different from Report)

NA

18. SUPPLEMENTARY NOTES

The view, opinions, and/or findings contained in this report are those of the author(s) and should not be construed as an official Department of the Army position, policy, or decision, unless so designated by other documentation.

19. KEY WORDS (Continue on reverse side if necessary and identify by block number)

dissociation, unimolecular, spin-orbit, spectroscopically, ionization, collisions.

20. ABSTRACT (Continue on reverse side if necessary and identify by block number)

Experimental results are presented wherein nascent PO($X^2\pi_i$) is detected following the collision-free infrared multiple photon excitation and dissociation of several volatile organophosphorus molecules which lead to PO via a sequence of bond fission reactions.

DTIC FILE COPY

DD FORM 1 JAN 73 1473 EDITION OF 1 NOV 65 IS OBSOLETE

UNCLASSIFIED

SECURITY CLASSIFICATION OF THIS PAGE (When Data Entered)

ARO 19095.3-CH

THE BIMOLECULAR REACTIONS OF OXIDIZING AGENTS WITH FREE RADICALS OF THE FORM PX: THE ROLE OF COMPLEX NUCLEAR MOTION

Jim-Son Chou, David S. Sumida and Curt Wittig

May 1, 1982 - April 30, 1985

U.S. ARMY RESEARCH OFFICE

DOCUMENT FUNDING NUMBER DAAG29-82-K-0118

University of Southern California

Los Angeles, CA 90089-0484

TABLE OF CONTENTS

I. INTRODUCTION

Dissociation processes which lead to fragments of $^2\Pi$ electronic character are interesting and of fundamental scientific importance. For example, selective excitation of one of the product Λ-doublets can reveal details of the dissociation with elegance and precision, and can allow spatial anisotropies to be perused within the molecular frame.[1-5] Also, spin-orbit interaction splits $^2\Pi$ into $^2\Pi_{1/2}$ and $^2\Pi_{3/2}$ components, and such states may correlate to quite distinct electronic states of the precursor, even though they are only separated by 10's or 100's of cm^{-1}. In fact, the literature contains many examples in which photodissociation leads to nascent NO fragments whose spin-orbit states are populated selectively,[6,7] and this is often attributed to adiabatic correlations along separate electronic potential surfaces. Non-adiabatic couplings may decrease, or even change the selectivity,[8,9] so that it is not straightforward to surmise the respective roles of more than one potential surface from the observed selectivity. Since spin-orbit interaction removes part of the degeneracy of $^2\Pi$ states, it can influence surface crossings as well as affect energetics, and it will be important to measure nascent distributions for systems which involve a minimum number of potential surfaces (ideally, just one), in order to gain enlightenment about the elementary processes involved.

Dissociation events which transpire on the ground electronic potential surface, hereafter referred to as S_0, are particularly significant because of the importance of recombination and

unimolecular reactions in modern physical chemistry.[10,11] Selectivity for $^2\Pi_{1/2}$ or $^2\Pi_{3/2}$, if it exists, must be accounted for separately in any statistical theory of unimolecular processes, since such selectivity is of electronic origin, and the basic structure of such statistical theories involves randomizing nuclear degrees of freedom on a single electronic potential surface.[10,11] Thus, if vibrational predissociation on S_0 shows high selectivity toward a single spin-orbit state, it is hard to justify a treatment of either dissociation or recombination processes which simply assigns an electronic degeneracy to the $^2\Pi$ species.

In this paper, we present experimental results wherein nascent PO($X^2\Pi$) is detected following the collision-free infrared multiple photon excitation and dissociation (IRMPE and IRMPD) of several volatile organophosphorus molecules which lead to PO via a sequence of bond fission reactions. It is well known that IRMPD follows the lowest energy pathways for unimolecular decomposition, and that species are usually excited to energies such that the rate of optical pumping is balanced by the rate of unimolecular reaction.[12,13] Because of this, excited ensembles are not monoenergetic, but are spread over a modest energy range.[14] Sequential dissociations, in which decomposition products are themselves dissociated via IRMPD, are not special, and still follow the lowest energy pathways.[15,16] Thus, in using IRMPD to prepare PO($X^2\Pi$), we insure that this species derives from a precursor which is vibrationally excited, but in its electronic ground state.

PO($X^2\Pi$) is similar to NO($X^2\Pi$) in many respects. The spin-orbit splittings are small (224 and 123 cm^{-1} respectively), and therefore observed differences cannot be ascribed simply to energy. IRMPD typically promotes species to energies which are high enough above reaction threshold so that nascent products contain significant vibration, rotation, translation (V,R,T) excitation, and the 123 and 224 cm^{-1} spin-orbit excitations can be easily detected spectroscopically if they are present. The larger mass and spin-orbit interaction generate a Hund's case (a) coupling scheme for PO($X^2\Pi$), unlike the intermediate coupling scheme for NO($X^2\Pi$), so that correlations which select a single spin-orbit state may be seen more clearly, and this constitutes an advantage of using PO. rather than NO, to study such processes. As with NO, PO can be detected with high sensitivity by using multiphoton ionization (MPI). However, unlike NO, PO can be ionized via 2-photon MPI, using rather convenient laser wavelengths. The PO $B^2\Sigma^+ \leftarrow X^2\Pi$ system can be excited in the region 305-330 nm, and the subsequent absorption of a 266 nm photon causes ionization. The required laser energies are modest ($\lesssim$ 100's of μJ) and the signals vary linearly with each laser fluence and only occur with both beams present, thereby insuring a sensible and straightforward detection process.

In all of our experiments to date, we find an overwhelming propensity to form PO($X^2\Pi_{1/2}$), but not PO($X^2\Pi_{3/2}$). It seems clear that the species producing PO correlates adiabatically to the $^2\Pi_{1/2}$ state, but that the $^2\Pi_{3/2}$ state is inaccessible except via non-adiabatic processes. We expect these results to be quite general, and similar considerations should be made for a number of systems.

II. EXPERIMENTAL ARRANGEMENT

Molecular ions were detected using a laser time-of-flight mass spectrometer (TOFMS),[17] consisting of a double grid ionization region, a drift tube, and a tandem microchannel plate detection assembly (3×10^{-6} and 6×10^{-8} Torr in the ionization and detection regions respectively). Freshly distilled samples, from a separate gas handling system, were admitted through a variable leak valve into the ionization region, producing a constant sample pressure of $\sim 10^{-5}$ Torr. The output from a CO_2 TEA laser, operating in the 10.6 μm band, was focused into the ionization region of the TOFMS and produced nascent $PO(X^2\Pi)$ fragments, which were subsequently excited and ionized, nominally 350 ns after the onset of the counterpropagating CO_2 laser pulse. The cations thus produced entered the drift tube and were detected using the microchannel plate array. Signals were amplified, digitized (10 ns resolution), and sent to a microcomputer (LSI 11/23) for data processing. Photodiodes monitored the UV radiations, thereby providing normalization of the mass resolved PO^+ ion signal.

The detection scheme is shown schematically in Fig. 1. Tunable UV radiation (305-330 nm) was obtained using a tracking doubler and tunable dye laser, and 266 nm radiation was the 4th harmonic of the 1.06 μm Nd:YAG fundamental. For the medium resolution spectra, the dye laser cavity (i.e. air-spaced Fabry-Perot etalon and grating) was pressure tuned using 300-1500 Torr of N_2

for each scan. Scanning was done in 2 Torr increments, using a servomechanism controlled valve system (Datametrics) in conjunction with the microcomputer. The linewidth of the doubled dye laser was approximately 0.08 cm^{-1}. The unfocused UV beams were combined collinearly with a dichroic beamsplitter and an optical delay of 10 ns precluded simultaneous absorption of both photons. The laser energies were $\leq 100\,\mu J$ and the ion signal disappeared with either the 266 nm, tunable UV, or 10.6 μm radiation blocked. The CO_2 laser fluence was ~ 40 J cm^{-2} at the focal point.

In establishing that the MPI spectral signature is an exact replica of the $B^2\Sigma^+ \leftarrow X^2\Pi$ absorption spectrum, one must show that the 266 nm photon promotes the excited diatom into a structureless region of the ionization continuum. To verify that such is the case, a microwave discharge flow system was developed to produce PO in a thermalized environment. The flow system is constructed primarily from pyrex and quartz. The MPI ion current is monitored with two nickel wire electrodes, separated by 1 cm and biased with 180 volts. Freshly distilled sample was combined with Ar carrier gas and passed through the microwave cavity (2450 MHz). The cavity was nominally 12 cm upstream from the electrodes. Quartz windows were sealed with O-rings to the cell and a capacitance manometer monitored pressure. Total pressures were ~ 1 Torr, insuring that PO is thermalized at the ambient temperature (300-450K), having undergone ~ 10^7 collisions between the discharge and detecting regions. However, these pressures are still sufficiently low that molecules promoted to

the $B^2\Sigma^+$ state undergo almost no collisions before being ionized, so that spectra obtained thus can be compared directly to those of nascent PO. The ion current was differentially amplified, digitized, sent to the microcomputer, and normalized as per the UV laser fluences. As before, the ion signal disappeared with any of the laser beams blocked, and varied linearly with UV fluences. In this calibration experiment, the MPI spectra reproduced very well the PO $B^2\Sigma^+ \leftarrow X^2\Pi$ absorption spectra,[19] thus verifying the frequency independence of the absorption of the 266 nm photon.

For other calibration purposes, PO MPI spectra were obtained using an atmospheric pressure flame arrangement (nominally 2400K), which is essentially the burner assembly from an atomic absorption spectrometer with electrodes added in order to collect ions.[17]

The various organophosphorus compounds used are listed in Table I, and were obtained from Aldrich. DMMP (97%) and DIMP (98%) were purified to > 99% by fractional distillation. DMP (97%), DIP (95%), and TMP (99+%), were used without further purification. All compounds were degassed at 77K prior to use.

III. RESULTS

PO Electronic Energy Distribution ($^2\Pi_{1/2}$, $^2\Pi_{3/2}$)

Figure 2b shows a 2-frequency 2-photon ionization spectrum of nascent PO which derives from the collision-free IRMPD of dimethyl methylphosphonate (DMMP), in the region of the (0,0) and (1,1) bands of the $B^2\Sigma^+ \leftarrow X^2\Pi$ system. At all laser frequencies, PO^+ was the dominant ion in the mass spectra, and we had to increase the detection sensitivity by 4 orders of magnitude in order to observe other ions, which derived mainly from the non-resonant MPI of DMMP. No PO^+ signal was seen with the 10.6 μm radiation blocked, and as the probe was delayed relative to the onset of the CO_2 laser output, the PO^+ signal first rose and then decayed as the fragments left the ionization region.(17) The 266 nm radiation was delayed 10 ns relative to the tunable UV radiation in order to avoid processes involving the simultaneous annihilation of two photons, and to eliminate the possibility that the 266 nm radiation photolyzes any intermediates, thereby producing PO. To insure that the signals derived only from nascent PO, we studied the PO^+ signal as a function of the tunable UV laser fluence. If PO^+ indeed is born of PO, then the signal should vary linearly with the laser fluence. We do observe such linear behavior down to the smallest laser energies with which adequate signals could be obtained (1.5 μJ), thereby confirming that the PO^+ signals derive from nascent PO.

For the detection of PO downstream from the microwave discharge, the same 10 ns delay of the 266 nm radiation was used

as with the IRMPD case, and the same linear dependence of the ionization signal on the tunable UV laser fluence was observed. Figure 2a depicts the 2-frequency 2-photon ionization spectrum of PO detected in this 300K situation. Anderson et al.[20] observed LIF of PO in this spectral region using the same microwave discharge method, and both the rotational and spin-orbit states followed a 300K Boltzmann distribution. The 2-frequency 2-photon ionization spectrum shown in Fig. 2a duplicates the $B^2\Sigma^+ \leftarrow X^2\Pi$ absorption and LIF spectra,[19] and hence reflects the PO($X^2\Pi$) state distribution.

Comparing the MPI spectra of PO from collision-free IRMPD with those obtained using the microwave discharge, we confirm our previous observation[17] of the very low occupancy of the excited spin-orbit doublet (224 cm^{-1} above the ground $^2\Pi_{1/2}$ state), following collision-free IRMPD of DMMP. Were the $^2\Pi_{1/2}$ and $^2\Pi_{3/2}$ states assigned a temperature based on their relative populations, it would be approximately 150K, in marked contrast to the much higher vibrational and rotational excitations, which are typical for IRMPD.

A similar spin-orbit population pattern was observed in the higher vibrational states, using 1-frequency 2-photon ionization. The air/C_2H_2 flame created the high temperature environment necessary for a thermal distribution in $v''>0$ levels, thus serving as a reference for these spectra. Spectra of the (5,4) band region using both collision-free IRMPD and the flame are shown in Fig. 3. In the flame, the (5,4)($Q_{21}+R_{11}$), (5,4)($Q_{22}+R_{12}$), and (5,4)R_{22} bands are quite evident, whereas in the IRMPD

measurement the (5,4)R_{22} band is almost completely absent, and the intensity of the (5,4)(Q_{22}+R_{12}) band relative to the (5,4)(Q_{21}+R_{11}) band decreased by a factor of 7 compared to the flame result.

Further confirmation of the small PO($^2\Pi_{3/2}$) nascent populations was obtained by thermalizing the nascent PO using an inert diluent. In these experiments, the flow system provided the best environment, and results are shown in Fig. 4. Collisions efficiently populate the $^2\Pi_{3/2}$ state, as is seen from the increase in signal from the (0,0)(Q_{12}+P_{22}) band. The energy transfer rate is quite high, as in the case of NO,[21,22] and rate coefficients could be obtained if one were inclined to do so.

Absence of significant $^2\Pi_{3/2}$ excitation is not confined to DMMP, and a list of molecules which yield PO via IRMPD is given in Table I. In all cases, similar results were obtained, albeit with varying signal intensities, due to the different dissociation yields. An example of this is shown in Fig. 5, where nascent PO spectra are obtained using DMMP, TMP, DMP, and DIMP precursors. The similarity of these spectra is striking. The list of molecules in Table I is hardly exclusive; these were the only molecules tried, and we assume that other homologous species will yield similar results.

Rotational Energy Distribution in PO($^2\Pi_{1/2}$,v"=0)

With the dye laser system operating in the medium resolution mode (pressure scanning, 0.08 cm^{-1} resolution near 325 nm),

rotationally resolved spectra were obtained in the (0,0) P_1-branch for both collision-free IRMPD and the 300K effluent from the microwave discharge (see Fig. 6). The 300K reference sample appears completely thermalized, and the spectrum shown in Fig. 6b is the same as the one obtained using LIF of a 300K sample.[19] With IRMPD, nascent rotational excitation clearly exceeded 300K, but did not appear completely Boltzmann. The spectrum showed an interesting and repeatable peak at J=19.5. In order to further insure against artifacts, spectra were recorded using the more compacted R_1-branch and the results were qualitatively similar (e.g. rapid drop for J>19.5) to those shown in Fig. 6. Rotational populations are determined using linestrength factors which are calculated from formulae derived by Earls[23] (see the Appendix), and the populations thus obtained are given in Fig. 7. Figure 7b includes data obtained by Clyne et al.[19] using LIF, and the agreement with our MPI spectrum is excellent. Inadequate S/N prevented us from obtaining a rotationally resolved spectrum of the $B^2\Sigma^+ \leftarrow X^2\Pi_{3/2}$ (0,0) band following collision-free IRMPD. In simulating the unresolved rotational band contours of the systems shown in Fig. 2b, we find that a rotational 'temperature' of ~800K fits the data fairly well, but that such a fit is not unique. The uncertainty of this 'temperature' can be as high as ± 200K, and may reflect the non-Boltzmann character of the rotational distribution shown in Fig. 7.

Nascent PO($X^2\Pi_{1/2}$) Vibrational Excitation

Nascent vibrational excitation is evident following collision-free IRMPD of the molecules listed in Table I (see Figs. 2-5). Vibrational levels as high as v"=6 have been observed,[17] and the (1,1) band is in a region where quantitative estimates of the relative v"=0 and 1 populations can be made. In comparing the areas of the Q-branches, and scaling by the Franck-Condon factors, we find that [v"=1]/[v"=0] ≈ 0.17 for the data shown in Fig. 2b, in which DMMP is the precursor. Very similar results are obtained with the other precursors listed in Table I. Were a 'temperature' ascribed to v"=0 and 1, it would be approximately 1000K. Similar vibrational 'temperatures' were also extracted when comparing the signal intensities of the (5,4) and (6,5) bands, obtained using 1-frequency 2-photon ionization detection, following collision-free IRMPD of DMMP, with a 2400K flame for calibration.

Nascent PO($X^2\Pi_{1/2}$) Translational Excitation

Even with a resolution of 0.08 cm^{-1}, we find that spectra of nascent PO are Doppler broadened noticeably more than those of 300K thermalized samples, as shown in Fig. 8. It is very hard to derive velocity distributions from Doppler lineshapes under the best of circumstances, and with the S/N of the present experiments, such a deconvolution is impossible. We note that Maxwell-Boltzmann velocity distributions with temperatures of 1500-2000K, convoluted with the 0.08 cm^{-1} probe linewidth, reproduce the experimental linewidths. Such an estimate of the

average translational energy is the best that can be done without resorting to inherently more accurate molecular beam techniques.[25] This amount of nascent translational excitation is to be expected for a series of bond fission reactions, and is lower than would be expected for molecular eliminations.[26]

IV. DISCUSSION

Reaction Pathways for Producing PO($X^2\Pi$)

The production of PO($X^2\Pi$) by the collision-free IRMPD of the molecules listed in Table I proceeds sequentially, and involves the dissociation of nascent fragments via the lowest energy reaction pathways. Typical bond energies are listed in Table II, and using this information we conclude that the primary dissociation events produce radicals of the form $(RO)_2PO$, where R=CH_3 or i-C_3H_7. In the absence of molecular eliminations, the most likely immediate precursors of PO are of the form ROPO, which can then yield PO directly. Since the C-O and P-O bonds are of comparable strength, it is likely that PO_2 will be produced in addition to PO. However, the experimental results suggest that nascent PO does not derive from the IRMPD of PO_2. Such a small species would dissociate as soon as it acquired energy in excess of reaction threshold, thereby producing PO without vibrational excitation, in marked contrast to our observations. Thus, the production of PO($X^2\Pi$) can be rationalized straightforwardly, using a mechanism which involves 3 sequential dissociation steps.

PO($X^2\Pi_{1/2}$) Favored Over PO($X^2\Pi_{3/2}$)

By far, the most intriguing of the results presented above is the small population of the upper PO($X^2\Pi$) spin-orbit doublet, $^2\Pi_{3/2}$, which lies only 224 cm^{-1} above the $^2\Pi_{1/2}$ electronic ground

state. This result is unambiguous. It persists with all of the precursors listed in Table I and with different CO_2 laser fluences, and it is verified using PO obtained from microwave discharges and flames, and by adding an inert buffer gas in order to thermalize (300K) the nascent $PO(X^2\Pi)$ produced via IRMPD.

Since distinct electronic potential surfaces correlate to the $^2\Pi_{1/2}$ and $^2\Pi_{3/2}$ species, one must consider carefully the parentage of these excitations. IRMPE prepares excited molecules whose vibrations can be considered random in a normal mode description, and product V,R,T distributions can be estimated rather well using statistical theories such as the separate statistical ensemble (SSE) formulation of the phase space theory of unimolecular reactions (PST), for dissociations involving loose transition states.[28] However, there is no a priori reason to assume that electronic excitations are randomized with the nuclear degrees of freedom, and non-adiabatic couplings may be required in order to randomize electronic and nuclear degrees of freedom. Electronic specificity deriving from spin conservation has been noted in several systems,[16,29] and spin-orbit states can also be produced with specificity, since the multiplets needn't all correlate with the ground state surface of the precursor.[30-32] Each of the product spin-orbit states contain angular momenta which, when combined with the angular momenta of the other fragment, correspond to distinct potential surfaces of the species undergoing dissociation. Thus, specificity with respect to product electronic states is to be expected, even for

as democratic a process as IRMPD. We note that such considerations are also germane to recombination, wherein certain formalisms require that electronic partition functions be assigned values.[33,34]

Based on recent **ab initio** calculations of HPO,[35] as well as analogy with species such as NO_2, HNO, NCNO, NOBr, NOCl, CF_3NO, etc., many species containing the PO group are expected to have an excited singlet state (A^1A'', hereafter referred to as S_1) near or below the dissociation threshold. In these cases, non-radiative processes degrade initial S_1 electronic excitation, and dissociation products are detected when promoting molecules to energies in excess of reaction threshold. S_0 is often thought to couple strongly to S_1, thereby implicating S_0 in the dissociation.[36] Although these conclusions are obtained from studies of the $S_1 \leftarrow S_0$ absorption systems, they apply directly to IRMPE as per microscopic reversibility. The character of the state which derives from the coupling of S_0 and S_1 is influenced by statistical factors, which favor S_0 overwhelmingly. Thus, in a region of high S_1 vibrational state density, species produced by IRMPE are mainly of S_0 character, with a small contribution from S_1, due to $S_0 \rightleftarrows S_1$ coupling. The phosphorus analogs should behave similarly, and therefore IRMPE can prepare molecules with mixed S_0 and S_1 character, due to the coupling between these states. Again, because of the respective vibrational state densities within each electronic manifold, the statistical weight of S_0 will exceed that of S_1 significantly, as pointed out previously.[37] Since the actual dissociation event is rather

rapid ($\sim 10^{-13}$ s), the $^2\Pi_{1/2}$ and $^2\Pi_{3/2}$ product states will be produced by motions on the surfaces correlating to these states, along with the concomitant non-adiabatic processes which occur as the system goes from near the precursor equilibrium geometry to the products. From our results, it seems very likely that $PO(X^2\Pi_{1/2})$ correlates with the ground electronic state of its immediate precursor and $PO(X^2\Pi_{3/2})$ does not. A similar situation has been established for the $F+H_2$ reaction, wherein only the lower spin-orbit component, $F(^2P_{3/2})$, reacts with H_2 to produce electronic ground state HF.[31] If $PO(X^2\Pi_{3/2})$ correlates with S_1, then the small amount of $^2\Pi_{3/2}$ follows straightforwardly from the small amount of S_1 character present in the excited molecules. In fact, considering the likely densities of states for the S_0 and S_1 manifolds, such a mechanism may have to be accompanied by non-adiabatic interactions in the exit channel in order to account for as much $^2\Pi_{3/2}$ as is observed.

If S_0 does not correlate with $PO(X^2\Pi_{3/2})$, the capacity for selective production of $PO(X^2\Pi_{1/2})$ is quite high and is compromised only by non-adiabatic couplings in the exit channel. Here, $^2\Pi_{3/2}$ would correlate to a higher excited state, as has been seen in the case of $F(^2P_{1/2}) + H_2$.[31] Thus, the electronic specificity observed in the present measurements is in qualitative accord with likely correlations between product $^2\Pi_{1/2}$ and $^2\Pi_{3/2}$ states and the immediate PO precursors. A careful examination of the literature reveals that nascent NO photoproducts display similar trends, with production via the S_0 state of a precursor favoring $^2\Pi_{1/2}$,[7] while production from

higher electronic states may favor $^2\Pi_{3/2}$.(6) We expect such trends to be quite general, and certainly as the $^2\Pi$ fragments approach the Hund's case (a) limit, the propensity for selective production of product spin-orbit states will become more evident.(38)

V,R,T Excitations

The sequential dissociation steps leading to PO($X^2\Pi$) each involve the collision-free IRMPD of a polyatomic species. The IRMPD process causes almost no change in parent translation, only modest changes in parent rotation,(39) and enough vibrational excitation so that unimolecular reaction is usually rapid on the time scale of the CO_2 laser pulse duration. Since vibrations are randomized at energies above reaction threshold, there is almost no memory for the nascent vibrational excitations of those fragments which continue to absorb radiation and dissociate. However, product rotations and translations are passed on from one dissociation event to the next, so that the PO($X^2\Pi$) R,T distributions reflect the series of events that produce this species.

In all of our experiments to date, PO($X^2\Pi$) vibrational excitation could be ascribed a 'temperature' of approximately 1000K. This estimate is based on several vibrational levels, and this vibrational 'temperature' does not vary much with precursor or laser fluence. As mentioned previously, the fact that levels as high as $v''=6$ are observed indicates that PO_2 cannot possibly be the sole precursor of PO. A species as small as PO_2 could not

be excited to energies so high above reaction threshold that these product states could be produced, since the optical pumping rate could not overcome the large unimolecular rates characteristic of small molecules above reaction threshold. Based on previous studies in which nascent vibrational excitation was observed following IRMPD, T_v ~ 1000K seems reasonable,[16,40] particularly considering the likelihood of a precursor of the form ROPO.

Nascent translational excitation was detected in the medium resolution experiments by observing Doppler broadening of the individual rotational lines, and although accurate distributions cannot be derived from the data, we note that a nascent translational temperature of 1500-2000K fits the data reasonably well. In previous experiments, we have shown that simple bond fission processes display a propensity for producing vibrational excitation which exceeds rotational and/or translational excitations.[40] Although exit channel barriers (e.g. molecular elimination) can produce specific product excitations, there is no evidence or reason to believe that exit channel effects play a role in the present experiments. Thus, we conclude that the sizable PO($X^2\Pi$) translational excitation simply derives from the sequential nature of the events leading up to its production. Energy in excess of reaction threshold is apportioned statistically, with relative translation of the fragments in the center of mass of the dissociating species receiving a democratic share of this energy. However, when the fragments thus produced are themselves dissociated, the resulting products again receive

translational excitation, so that translational energy accumulates during a sequence of dissociation events.

Nascent rotational excitation, as with nascent vibrational and translational excitations, is modest and consistent with a mechanism whereby PO is produced via a series of bond fission processes. From simulations of the low resolution spectra, rotational 'temperatures' of ~ 800K are obtained, and this seems reasonable in light of the medium resolution rotationally resolved spectra. We are presently unable to explain the peak in the rotational distribution at J=19.5. Despite modest S/N, this feature was quite persistent in all of the experiments. It is curious that the energy of the J=19.5 state is only slightly higher than that of the excited spin-orbit doublet, but this may be simply coincidence. Regardless, the average rotational energy is modest, and entirely consistent with the sequential dissociation mechanism.

V. SUMMARY

1. PO($X^2\Pi$) is produced by the collision-free IRMPD of volatile organophosphorous molecules such as those listed in Table I. Nascent V,R,T excitations are in accord with a sequence of bond fission reactions leading to the PO($X^2\Pi$) products, except for a few rotational levels near J=19.5, which are more populated than would be expected on statistical grounds. The most likely immediate precursor of PO is of the form ROPO.

2. There is an overwhelming propensity to favor the $^2\Pi_{1/2}$ state, even though $^2\Pi_{3/2}$ lies only 224 cm^{-1} higher. This persists under all experimental conditions, and is verified using 300K reference samples and when thermalizing nascent PO excitations using an inert buffer. Were an electronic 'temperature' ascribed to the nascent PO, it would be 150K.

3. This result underscores the importance of the separate electronic potential surfaces leading to the two PO spin-orbit states. It seems clear that $^2\Pi_{1/2}$ correlates with the electronic ground state of the immediate precursor to PO, and $^2\Pi_{3/2}$ does not. The small amount of $^2\Pi_{3/2}$ observed may be due to non-adiabatic transitions and/or 'freezing' the amount of S_1 character in a state of mixed S_0 and S_1 parentage.

4. We expect that such effects will be seen routinely when experimental conditions make such detailed scrutiny possible. Already, a careful look at nascent NO following photodissociation (often on S_0) suggests that selectivity toward specific spin-orbit states is present.

5. Because of microscopic reversibility, such selectivity must also be present in radical recombination reactions.

ACKNOWLEDGEMENT

We are indebted to C. McKenna and C. Chiu for providing samples and explaining the required handling and purification techniques, and we thank J. Tiee (LANL) for the loan of the air-spaced etalon.

APPENDIX

The Hönl-London factors for the (0,0) P_1-branch are given by the following expression[23]

$$\frac{(2J''+1)^2 + (2J''+1)\cdot(4J''^2+4J''+1-2\lambda(v''))\cdot\nu}{32J''}$$

where $\nu = \{\lambda^2(v'') - 4\lambda(v'') + (2J''+1)^2\}^{-1/2}$, $\lambda(v'') = \frac{A(v'')}{B(v'')}$,

and A(v") and B(v") are the spin-orbit splitting and rotational constants for the level v" respectively (A(v"=0)=224 cm^{-1},[41] B(v"=0)=0.73 cm^{-1} [42]). Several of these Hönl-London (HL) factors are listed below.

J	HL factor	J	HL factor	J	HL factor
0.5	0.0	10.5	1.41268	20.5	2.92833
1.5	0.16996	11.5	1.55717	21.5	3.08849
2.5	0.30790	12.5	1.70323	22.5	3.25019
3.5	0.44267	13.5	1.85086	23.5	3.41341
4.5	0.57748	14.5	2.00007	24.5	3.57817
5.5	0.71321	15.5	2.15086	25.5	3.74443
6.5	0.85018	16.5	2.30322	26.5	3.91220
7.5	0.98854	17.5	2.45716	27.5	4.08146
8.5	1.12839	18.5	2.61266	28.5	4.25221
9.5	1.26976	19.5	2.76972	29.5	4.42443

TABLE I. Molecules which produce PO by IRMPD, listed in order of decreasing dissociation yield.

NAME	MOLECULAR FORMULA	DISSOCIATION YIELD (arb. units)
Dimethyl Methylphosphonate (DMMP)	$(CH_3O)_2$ P(=O) CH_3	1.0
Trimethyl Phosphate (TMP)	$(CH_3O)_2$ P(=O) OCH_3	0.8
Dimethyl Phosphite (DMP)	$(CH_3O)_2$ P(=O) H	0.3
Di-isopropyl Methylphosphonate (DIMP)	$(i\text{-}C_3H_7O)_2$ P(=O) CH_3	0.04
Di-isopropyl Phosphite (DIP)	$(i\text{-}C_3H_7O)_2$ P(=O) H	<0.006

TABLE II. Typical bond energies (kcal mol^{-1}) of molecules such as those listed in Table I, taken from Ref. 27.

P-O	P-O	P-C	P-H	C-H	C-O
130	86	65	77	99	85

REFERENCES

1. F. Alberti and A.E. Douglas, Chem. Phys. **34**, 399 (1978).
2. A.M. Quinton and J.P. Simons, Chem. Phys. Lett. **81**, 214 (1981).
3. P. Andresen and E.W. Rothe, J. Chem. Phys. **78**, 989 (1983).
4. P. Andresen, G.S. Ondrey, E.Z. Titze, and E.W. Rothe, J. Chem. Phys. **80**, 2548 (1984).
5. R. Vasudev, R.N. Zare, and R.N. Dixon, Chem. Phys. Lett. **96**, 399 (1983); J. Chem. Phys. **80**, 4863 (1984).
6. R.J.S. Morrison and E.R. Grant, J. Chem. Phys. **77**, 5994 (1982).
7. R.D. Bower, R.W. Jones, and P.L. Houston, J. Chem. Phys. **79**, 2799 (1983).
8. H. Bony, M. Shapiro, and A. Yogev, Chem. Phys. Lett. **107**, 603 (1984).
9. M. Shapiro and R. Bersohn, to be published.
10. W. Forst, Theory of Unimolecular Reactions (Academic, New York, 1973).
11. P.J. Robinson and K.A. Holbrook, Unimolecular Reactions (London: Wiley-Interscience, 1972).
12. E.R. Grant, P.A. Schulz, As.S. Sudbo, M.J. Coggiola, Y.T. Lee, and Y.R. Shen, in Laser Spectroscopy, ed. by J.T. Hall and J.L. Carlsten (Springer Verlag, 1977), Springer Series in Optical Science, Vol. 7.

13. M.N.R. Ashfold and G. Hancock, "Infrared Multiple Photon Excitation and Dissociation: Reaction Kinetics and Radical Formation," in Gas Kinetics and Energy Transfer, Vol. 4, ed. by P.G. Ashmore and R.J. Donovan (Royal Society of Chemistry, 1981).

14. H. Reisler, F. Kong, C. Wittig, J. Stone, E. Thiele, and M.F. Goodman, J. Chem. Phys. 77, 328 (1982).

15. A.J. Grimley and J.C. Stephenson, J. Chem. Phys. 74, 447 (1981).

16. M.H. Yu, M.R. Levy, and C. Wittig, J. Chem. Phys. 72, 3789 (1980).

17. J.S. Chou, D.S. Sumida, and C. Wittig, Chem. Phys. Lett. 100, 397 (1983).

18. J.M. Dyke, A. Morris, and A.Ridha, J. Chem. Soc. Farad. Trans. II 78, 2077 (1982).

19. M.A.A. Clyne and M.C. Heaven, Chem. Phys. 58, 145 (1981).

20. W.R. Anderson, S.W. Bunte, and A.J. Kotlar, CLEO Meeting, Baltimore, MD. (May 1983).

21. Y. Nachshon and P.D. Coleman, J. Chem. Phys. 61, 2520 (1974).

22. Aa. Sudbo and M.M.T. Loy, Chem. Phys. Lett. 82, 135 (1981); J. Chem. Phys. 76, 3646 (1982).

23. L.T. Earls, Phys. Rev. 48, 423 (1935).

24. R.J.M. Bennett, Mon. Not. R. Astr. Soc. 147, 35 (1970).

25. M.J. Coggiola, P.A. Schulz, Y.T. Lee, and Y.R. Shen, Phys. Rev. Lett. 38, 17 (1977).

26. Aa.S. Sudbo, P.A. Schulz, Y.R. Shen, and Y.T. Lee, J. Chem. Phys. 69, 2312 (1978).

27. D.E.C. Corbridge, "Phosphorus - An Outline of its Chemistry, Biochemistry, and Technology," (Elsevier, Amserdam, 1980), p. 24.

28. I. Nadler, H. Reisler, M. Noble, and C. Wittig, J. Chem. Phys., in press.

29. M.N.R. Ashfold, G. Hancock, G.W. Ketley, and J.P. Minshull-Beach, J. Photochem. 12, 75 (1980).

30. A.C. Luntz, A.W. Kleyn. and D.J. Auerbach, J. Chem. Phys. 76, 737 (1982); P. Andresen and A.C. Luntz, J. Chem. Phys. 72, 5842 (1980); A.C. Luntz and P. Andresen, J. Chem. Phys. 72, 5851 (1980).

31. J.C. Tully, J. Chem. Phys. 59, 5122 (1973).

32. J.T. Muckerman, J. Chem. Phys. 54, 1155 (1971); J.T. Muckerman and M.D. Newton, J. Chem. Phys. 56, 3191 (1972).

33. R.L. Jaffe and J.B. Anderson, J. Chem. Phys. 54, 2224 (1971).

34. D.G. Truhlar, J. Chem. Phys. 56, 3189 (1972).

35. M. Schmidt and M. Gordon, private communication.

36. M. Noble, I. Nadler, H. Reisler, and C. Wittig, J. Chem. Phys. (1984), in press.

37. H. Reisler and C. Wittig, "Electronic Luminescence Resulting from Infrared Multiple Photon Excitation," in Photo-selective Chemistry, Part I, ed., J. Jortner, R.D. Levine and S.A. Rice, in "Advance in Chemical Physics" Series, Vol. XLVII, gen. ed., I. Prigogine and S.A. Rice (Wiley, New York, 1981).

38. Let $\lambda = A/B$, where A is the spin-orbit coupling constant and B is the rotational constant, so that Hund's case (a) can be expressed as $\lambda \rightarrow \infty$ (A>>B). In this coupling situation, the orientation of the final spatial wavefunctions for both spin-orbit multiplets can be described by similar admixtures of symmetry elements (i.e. A' and A" in C_s symmetry). Thus, in correlating the precursor ground state to the lower spin-orbit component, correlations to the upper spin-orbit multiplet will be symmetry forbidden. For further discussion on the wavefunction orientation parameter, Δ, see W.D. Gwinn, B.E. Turner, W.M. Goss, and G.L. Blackman, The Astrophys. J. 179, 789 (1973) and M. Bertojo, A.C. Cheung, and C.H. Townes, The Astrophys. J. 208, 914 (1976).

39. J.B. Halpern, Chem. Phys. Lett. 67, 284 (1979).

40. H. Reisler, F. Kong, A.M. Renlund, and C. Wittig, J. Chem. Phys. 76, 997 (1982).

41. R.D. Verma and S.R. Singhal, Can. J. Phys. 53, 411 (1975).

42. K. Kawaguchi, S. Saito, and E. Hirota, J. Chem. Phys. 79, 629 (1983).

FIGURE CAPTIONS

1. Schematic diagram concerning the photoionization of PO($X^2\Pi$) via the $B^2\Sigma^+$ state, showing both the 2-frequency 2-photon ionization and the 1-frequency 2-photon ionization probe schemes. A single photon promotes molecules to the $B^2\Sigma^+$ state, from which a 266 nm photon induces ionization. Low $B^2\Sigma^+$ vibrational levels cannot be ionized via a 1-frequency 2-photon process, but higher vibrational levels can, as shown in the diagram. The ionization potential is from ref. 18.

2. Low resolution 2-frequency 2-photon ionization spectra of $v''=0$ and 1. In (a), the sample is thermalized at 300K by detecting the PO 12 cm downstream from the microwave discharge where it is produced. In (b), nascent products are detected following collision-free IRMPD of DMMP. Note the small amount of PO($X^2\Pi_{3/2}$), as seen from the weak (0,0)($Q_{12}+P_{12}$) transition. In both instances, the 266 nm photon is delayed 10 ns relative to the tunable UV photon, and in the IRMPD situation, the CO_2 laser onset precedes the tunable UV laser onset by 350 ns. Even though individual rovibronic transitions are unresolved, the different E,V,R energy distributions for the thermal and nascent PO are apparent (see text).

3. Low resolution 1-frequency 2-photon ionization spectra of PO: (a) in an air/acetylene flame, and (b) from the collision-free IRMPD of DMMP. The spectra are not corrected for laser energy variation, which decreases by 10% from 320 to 318 nm. The (5,4)(Q_{22}+R_{12}) and (5,4)R_{22} bandheads originate from the upper spin-orbit component of the ground state, whereas the other identified features are from the lower spin-orbit state. Note the "colder" electronic distribution in the IRMPD case as evidenced by the decrease of the (5,4)(Q_{22}+R_{12}) band relative to the (5,4)(Q_{21}+R_{11}) band and the nearly complete absence of the (5,4) R_{22} band. In (b), the CO_2 laser onset precedes the tunable UV laser by 350 ns.

4. 2-frequency 2-photon ionization signal vs. tunable UV wavelength for different DMMP/buffer gas mixtures. The timing of the IR and UV laser pulses is described in the text. Note the rapid thermalization (300K) of the nascent electronic excitation, compared to vibrational excitation, as the buffer gas pressure is increased from 0 to 1000 mTorr.

5. 2-frequency 2-photon ionization signals vs. tunable UV wavelength, for the collision-free IR laser photolysis of different organophosphorus compounds: (a) DMMP, (b) TMP, (c) DMP, and (d) DIMP. Spectra (a)-(d) differ in their respective vertical scales and are listed in order of decreasing dissociation yield as per Table I. No MPI spectra of DIP were recorded, due to the low PO yield.

Typical operating pressures vary from 10^{-5}-10^{-4} Torr for these samples. Note the striking similarity of the PO($X^2\Pi$) E,V,R energy distributions for the different starting materials.

6. Rotationally resolved PO $B^2\Sigma^+ \leftarrow X^2\Pi_{1/2}$ spectra (0.08 cm^{-1} resolution) obtained via 2-frequency 2-photon ionization: (a) following the collision-free IRMPD of DMMP, and (b) using the 300K effluent from the microwave discharge. The dashed lines correspond to Boltzmann distributions, calculated using the formulae given in the appendix.

7. PO($X^2\Pi_{1/2}$,v"=0) rotational state distributions from: (a) the collision-free IRMPD of DMMP, and (b) 300K samples. Note the agreement between the 300K ionization (this work) and LIF (Clyne et al.)[19] results. The rotational energy was calculated as per ref. 24, which provides a closed form expression for any intermediate coupling situation between Hund's cases (a) and (b).

8. Spectra showing Doppler broadening due (a) to nascent (PO($X^2\Pi_{1/2}$) translational excitation, and (b) to a 300K reference sample. Despite the modest S/N, the PO $B^2\Sigma^+ \leftarrow X^2\Pi_{1/2}$ spectra obtained following collision-free IRMPD are clearly broader than those obtained using a 300K sample. The laser bandwidth is 0.08 cm^{-1}.

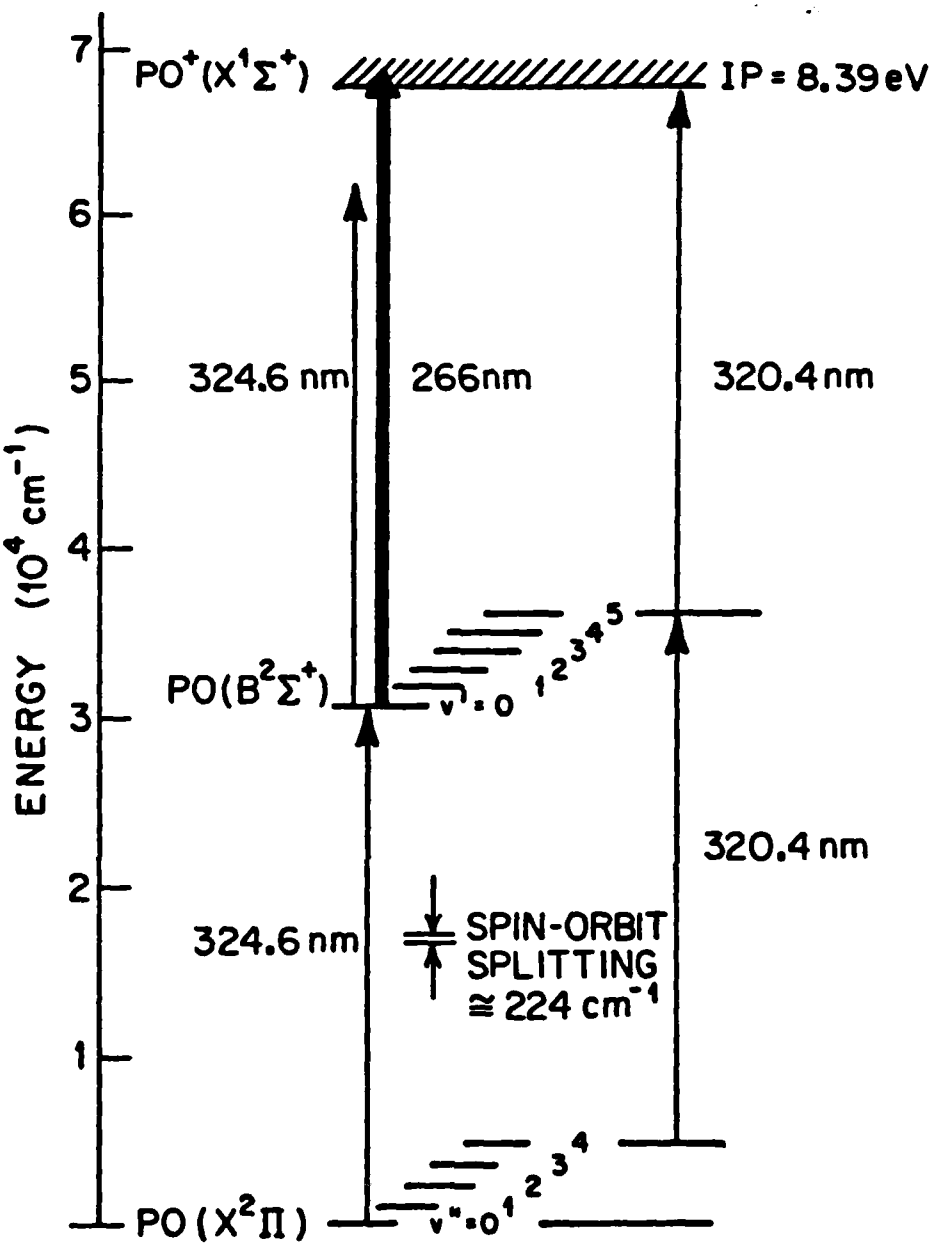
7
6
5
4
3
2
1
ENERGY (10^4 cm^{-1})
PO$^+$($X^1\Sigma^+$)
IP = 8.39 eV
324.6 nm
266nm
320.4nm
PO($B^2\Sigma^+$)
v' = 0 1 2 3 4 5
320.4 nm
324.6 nm
SPIN-ORBIT SPLITTING ≅ 224 cm^{-1}
v'' = 0 1 2 3 4
PO($X^2\Pi$)

#1

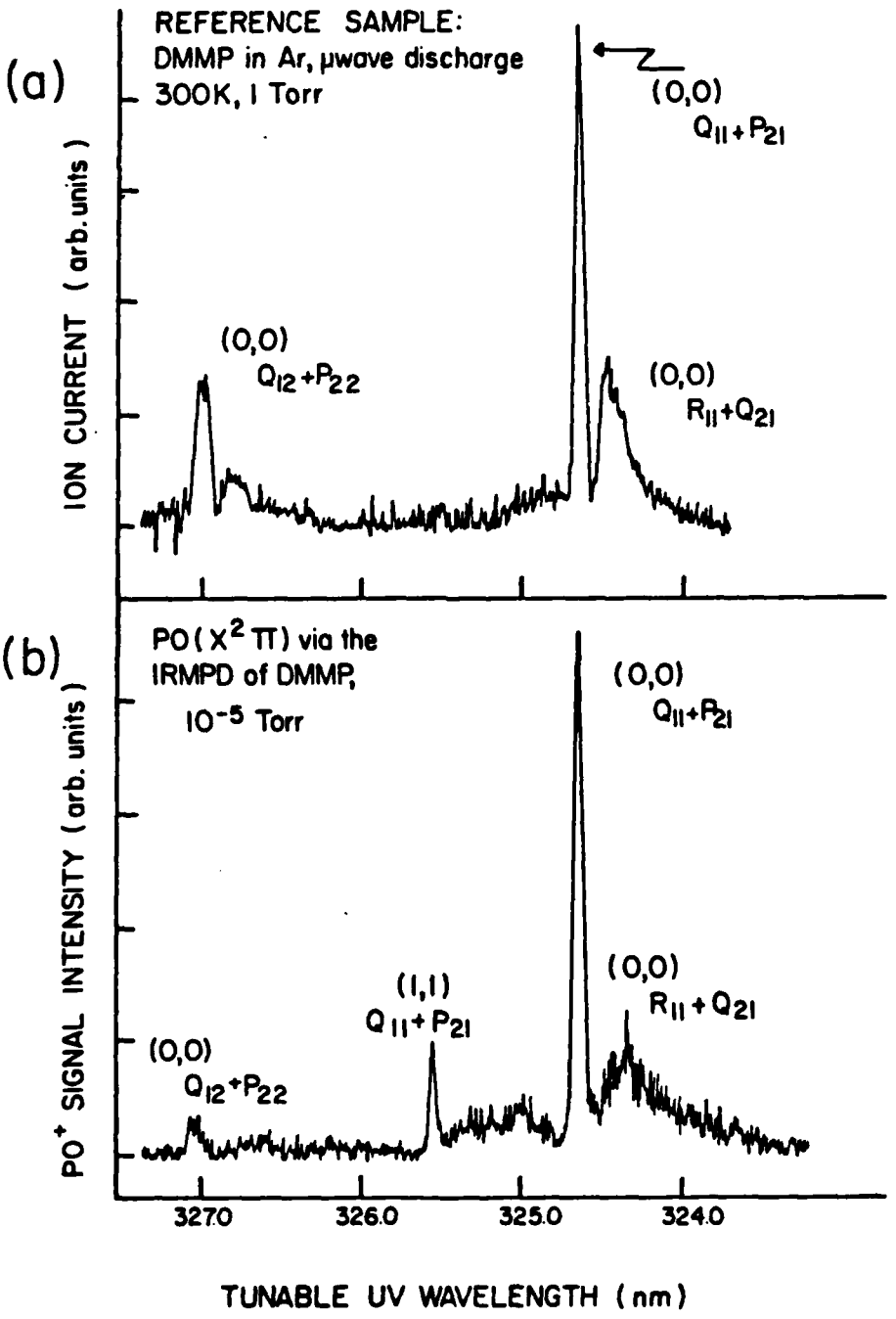
(a)
REFERENCE SAMPLE:
DMMP in Ar, μwave discharge
300K, 1 Torr
(0,0)
$Q_{11}+P_{21}$
(0,0)
$Q_{12}+P_{22}$
(0,0)
$R_{11}+Q_{21}$
ION CURRENT (arb. units)
(b)
PO($X^2\Pi$) via the
IRMPD of DMMP,
10^{-5} Torr
(0,0)
$Q_{11}+P_{21}$
(1,1)
$Q_{11}+P_{21}$
(0,0)
$R_{11}+Q_{21}$
(0,0)
$Q_{12}+P_{22}$
PO^+ SIGNAL INTENSITY (arb. units)
327.0
326.0
325.0
324.0
TUNABLE UV WAVELENGTH (nm)

#2

1- FREQUENCY PO MPI SPECTRA

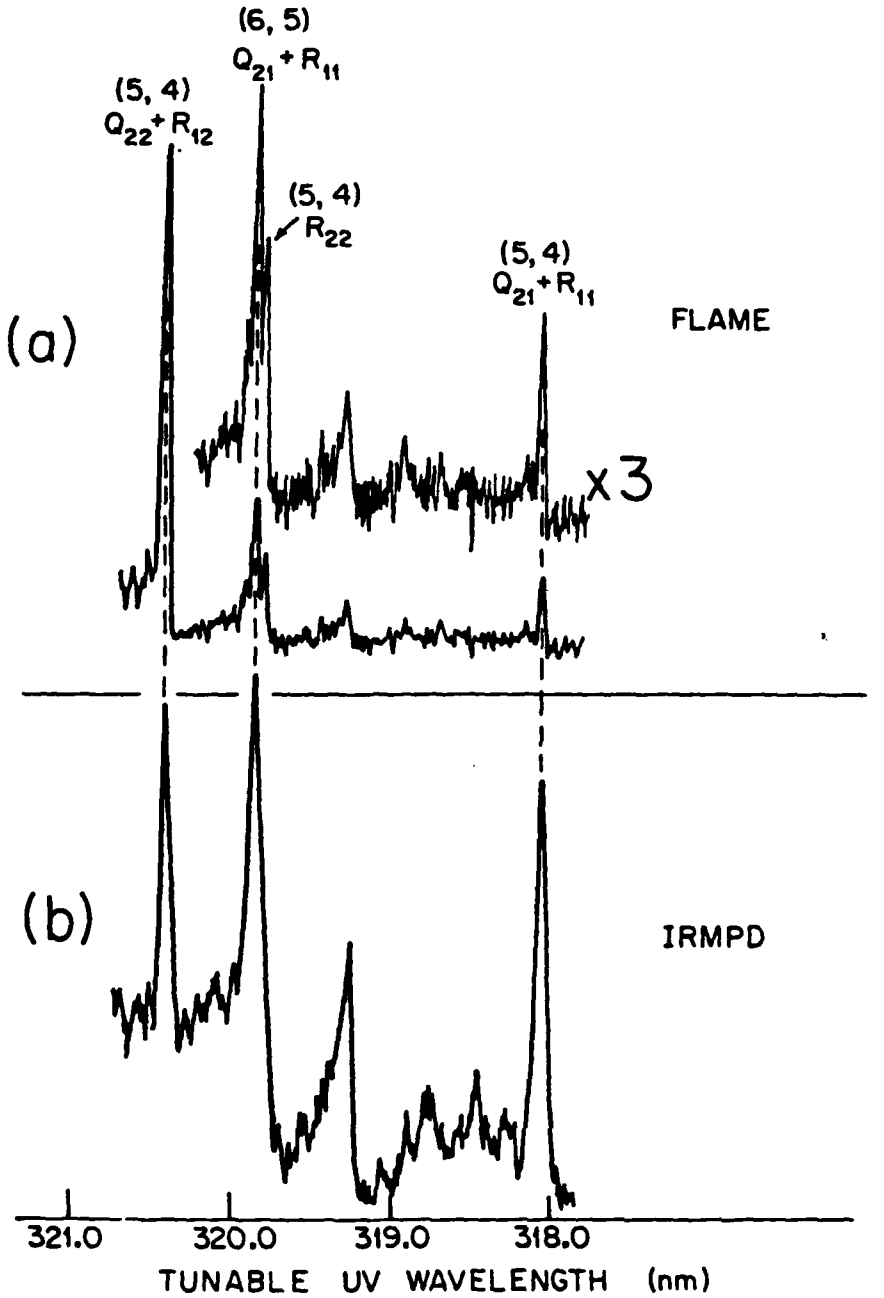

#3

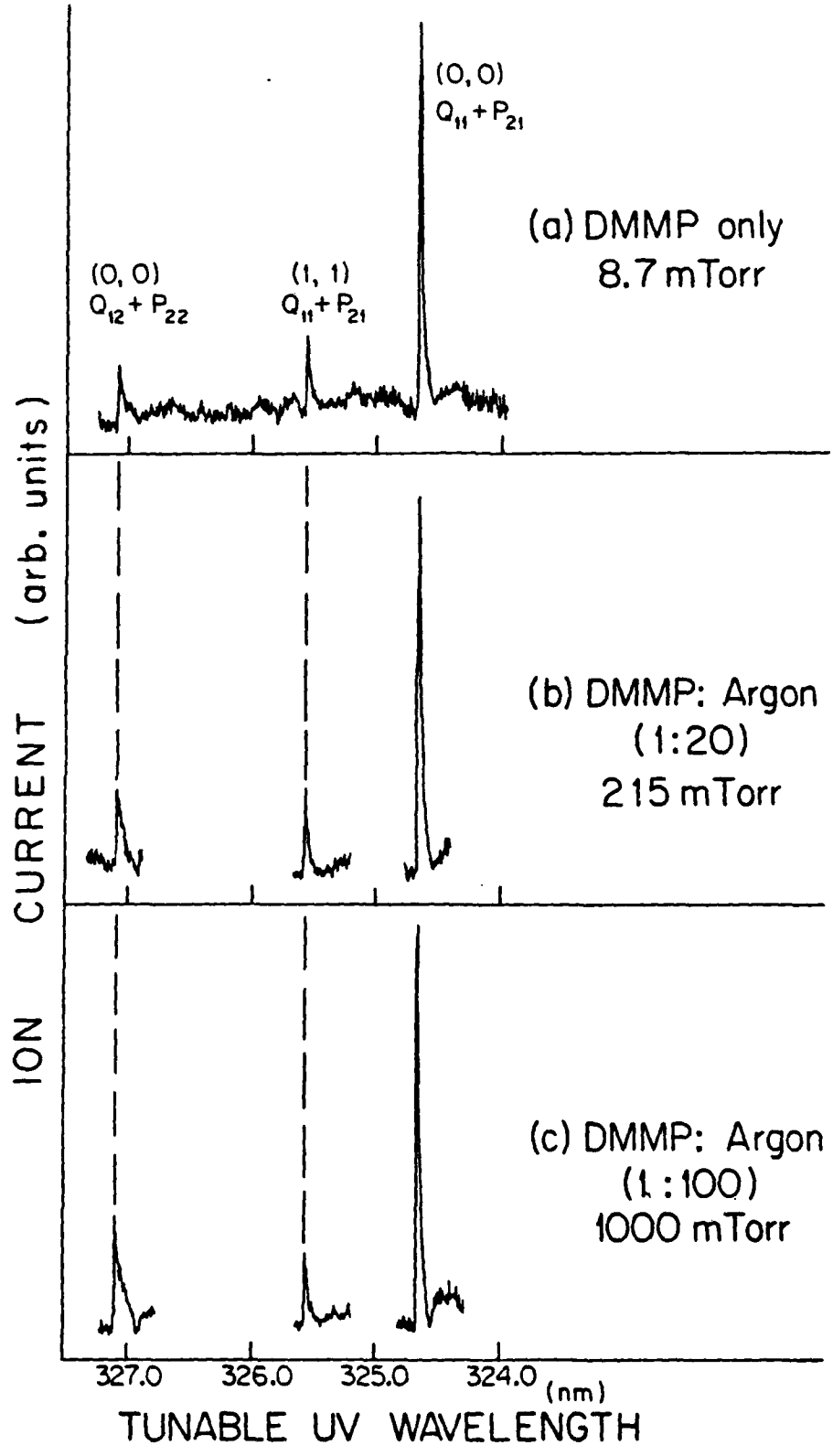
(0, 0)
$Q_{11} + P_{21}$
(a) DMMP only
8.7 mTorr
(0, 0)
$Q_{12} + P_{22}$
(1, 1)
$Q_{11} + P_{21}$
(b) DMMP: Argon
(1:20)
215 mTorr
(c) DMMP: Argon
(1:100)
1000 mTorr
ION CURRENT (arb. units)
327.0
326.0
325.0
324.0
(nm)
TUNABLE UV WAVELENGTH

#4

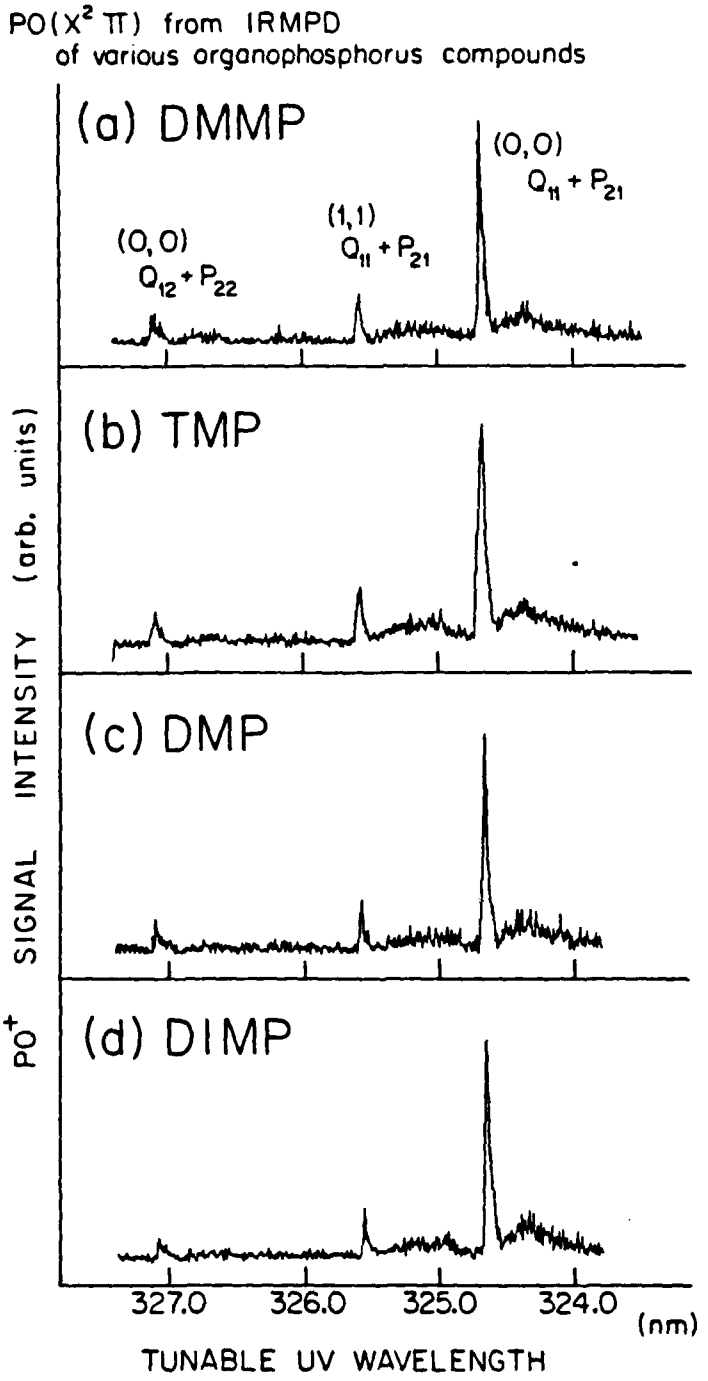
PO($X^2\Pi$) from IRMPD
of various organophosphorus compounds
(a) DMMP
(0,0)
$Q_{11} + P_{21}$
(1,1)
$Q_{11} + P_{21}$
(0,0)
$Q_{12} + P_{22}$
(b) TMP
(c) DMP
(d) DIMP
PO^+ SIGNAL INTENSITY (arb. units)
327.0
326.0
325.0
324.0
(nm)
TUNABLE UV WAVELENGTH

#5

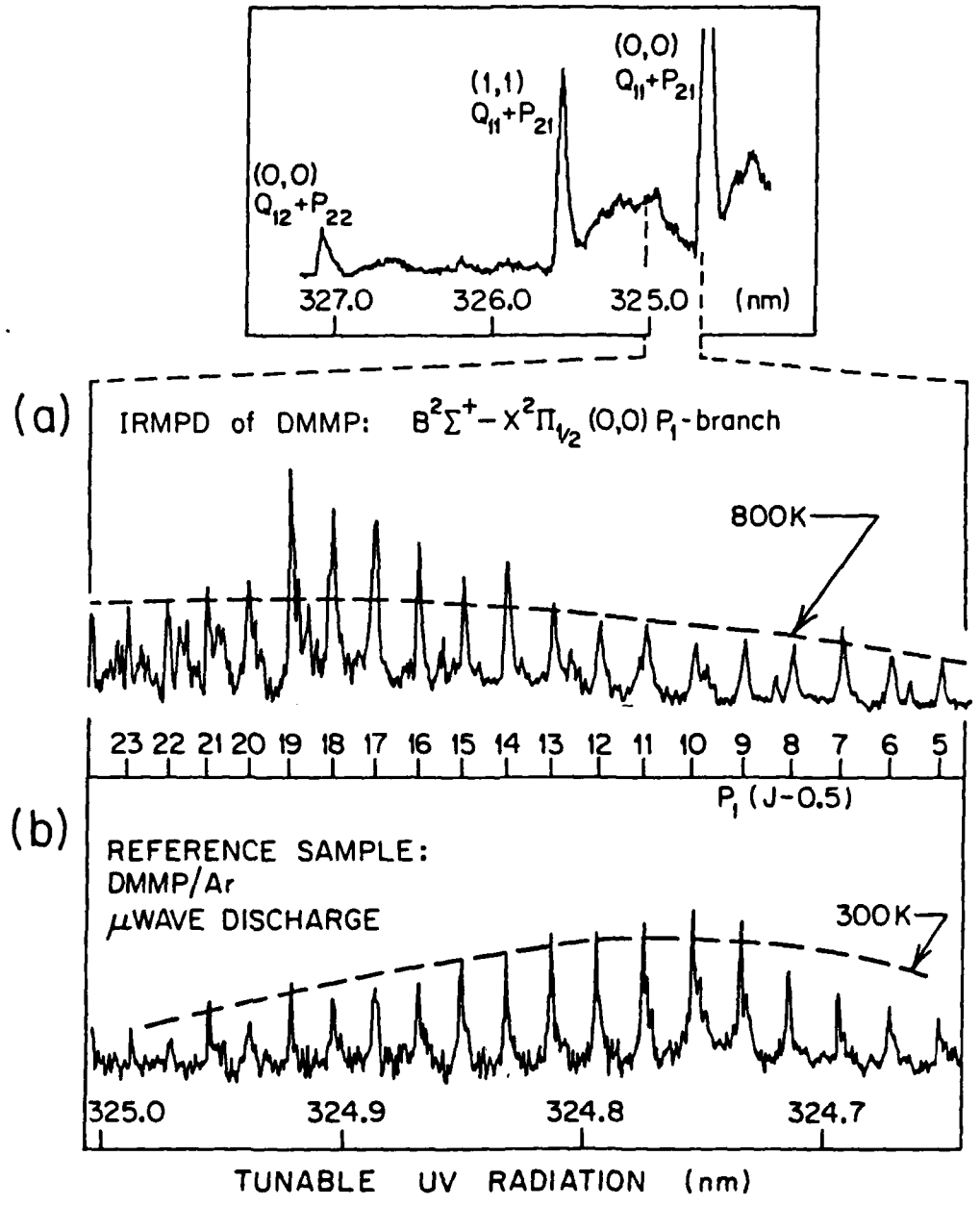
(0,0)
$Q_{12}+P_{22}$
(1,1)
$Q_{11}+P_{21}$
(0,0)
$Q_{11}+P_{21}$
327.0
326.0
325.0
(nm)
(a)
IRMPD of DMMP: $B^2\Sigma^+ - X^2\Pi_{1/2}$ (0,0) P_1-branch
800K
23 22 21 20 19 18 17 16 15 14 13 12 11 10 9 8 7 6 5
P_1 (J-0.5)
(b)
REFERENCE SAMPLE:
DMMP/Ar
μWAVE DISCHARGE
300K
325.0
324.9
324.8
324.7
TUNABLE UV RADIATION (nm)

#6

PO $B^2\Sigma^+ - X^2\Pi_{\frac{1}{2}}$ (0,0) P_1 BRANCH

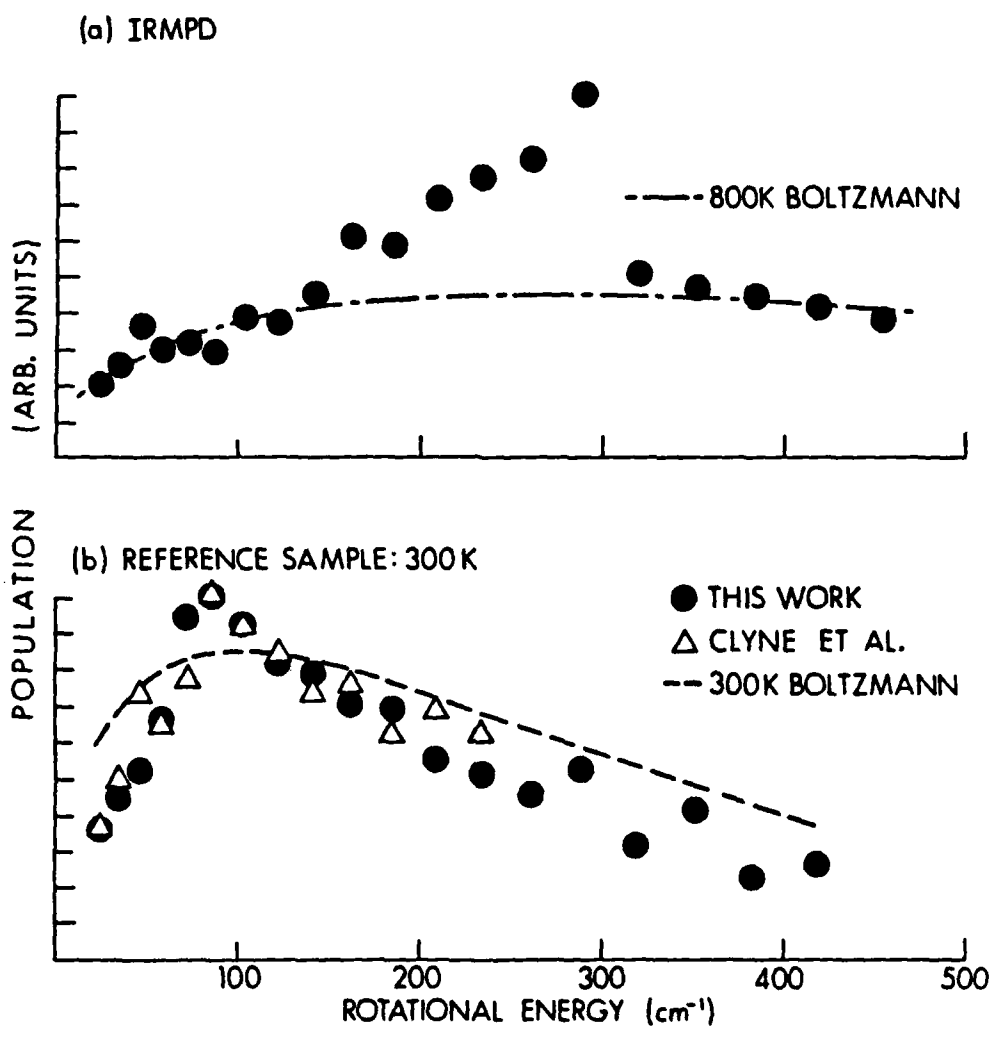

#7

PO $B^2\Sigma - X^2\Pi_{\frac{1}{2}}(0,0)$ P_1 BRANCH

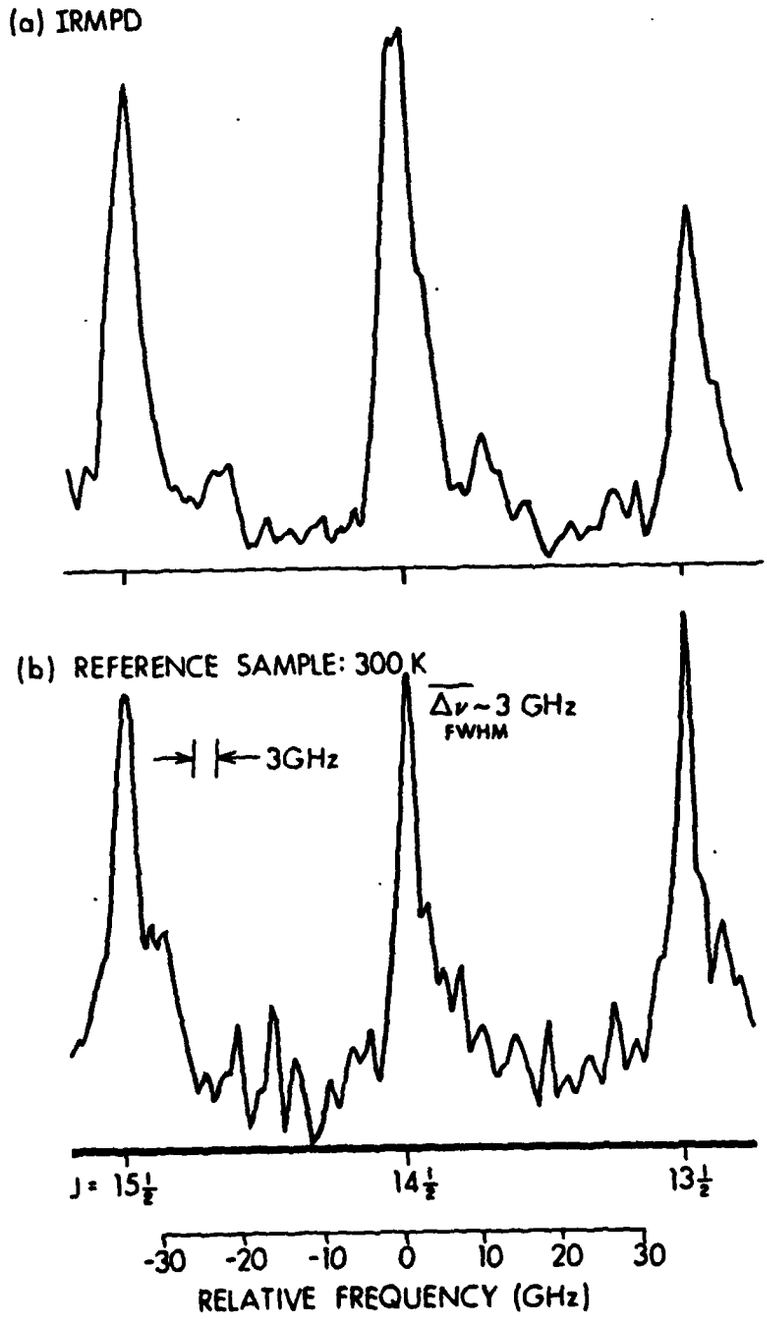

#8

LIST OF MANUSCRIPTS SUBMITTED OR PUBLISHED UNDER ARO SPONSORSHIP DURING THIS REPORTING PERIOD, INCLUDING JOURNAL REFERENCES

1. "Two-frequency two-photon ionization of nascent PO(X^2) from the collision-free IR photolysis of dimethyl methylphosphonate," J.S. Chou, D.S. Sumida and C. Wittig, Chem. Phys. Lett. **100**, 397 (1983).

2. "Stepwise excitation processes in photodissociation and detection," H. Reisler, G. Radhakrishnan, D. Sumida, J. Pfab, J.S. Chou, I. Nadler, and C. Wittig, Israel J. Chem. **24**, 229 (1984).

3. "Nascent PO(X^2) E.V,R,T excitations from collision-free IR laser photolysis: Specificity toward the PO(X^2) spin-orbit state," J.S. Chou, D. Sumida, and C. Wittig, J. Chem. Phys. **82**, 1376 (1985).

SCIENTIFIC PERSONNEL SUPPORTED BY THIS PROJECT AND DEGREES AWARDED DURING THIS REPORTING PERIOD

Curt Wittig

Jim-Son Chou

David S. Sumida (Ph.D., September 1984)

END

FILMED

3-86

DTIC